The Effect of Ion Beam Etching on Mechanical Strength Multilayer Aluminum Membranes

Evgeney E. Gusev, Anna V. Borisova, Anna A. Dedkova, Anton A. Salnikov and Valeri Yu. Kireev
National Research University of Electronic Technology «MIET»
Zelenograd, Moscow, Russia
bubbledouble@mail.ru

***Abstract*—Experimental study of aluminum membranes on a silicon substrate was conducted. Different combinations of Al layers were formed by magnetron method. Thickness has been determined by scanning electron microscope and secondary ion mass spectrometer. The distribution of atoms in the depth of the material was shown. The border between single layers of aluminum was detected. The dependence of the surface roughness on the number of membrane layers was given. A method for assessing the mechanical strength of circular membranes has been developed. Influence of ion beam etching process on membrane mechanical strength investigated.**

Keywords— mechanical strength; mechanical stresses; thin films; membranes; MEMS; ion beam etching

I. INTRODUCTION

Micro and nanotechnology membrane often plays a key role in sensors (MEMS devices). The membrane is a part of film, that is located in the air on part of it on the substrate. The membrane is part of the anode in x-ray sources [1,2,3]. It is a converter of electron energy into photon energy. On the other way, it is a part of sensitive element in gas flow meters [4,5,6]. The size of focal spot and x-ray intensity are increasing, while increasing the area of the membrane. Measurement area is increasing for air flow sensor. On the other hand, mechanical strength of structure is decreasing. That's why the amount of overpressure that the structure can withstand without breaking is decreasing. Besides, the probability of destruction when exposed to the electrons of the anode [7] or the detection of high speeds of air flow is increasing. Mechanical properties of bulk and film materials are different [8,9]. Therefore, the metrological base for controlling the mechanical strength of membranes needs to be developed.

The mechanical strength of the membranes was measured by contact (using an indenter [9, 10]) and contactless (forming an excess pressure by air flow [8]) methods.

One of the ways to increase the mechanical strength is the transition from a rectangular to a circular membrane [12]. This is due to the fact that membrane rupture occurs along the membrane-substrate boundary in most cases. The shape of the circle provides significantly lower values of elastic deformations compared to the rectangular shape of the membrane. The strain values are evenly distributed along the contour of the membrane and in the material of the membrane [12].

Another approach is to change the structure by reducing the grain size [9]. Increase in strength and hardness with a decrease in grain size due to the introduction of additional grain boundaries with large grain sizes, which are obstacles to the movement of dislocations. And increase in strength due to the low density of existing dislocations and the difficulty of forming new dislocations with nanoscale grains. The microhardness of nanocrystalline materials is 2-7 times higher than the hardness of coarse-grained analogues and it does not depend on the method of obtaining material [9,13]. In a number of works, a decrease in hardness was observed with a decrease in the grain size below a certain critical size, which is associated with an increase in the fraction of triple junctions of grain boundaries [14].

But, experimental confirmation of the claimed effects practically absent in studies (including [9,12]) due to the lack of measuring stands. In this paper, the authors used ion beam etching to modify the crystal structure of the surface of a layer, and experimentally evaluated the effect of the process on the mechanical strength of the layers.

II. METHOD FOR ASSESSING MECHANICAL STRENGTH OF MEMBRANES

We had developed a method for assessing the mechanical strength of circular membranes. An equation is established between excess pressure on membrane P and maximum mechanical stress σ_{max}. The derivation of the equation is shown below (1)-(12). The value of mechanical stresses σ is calculated as root of the sum of squares of radial σ_r and tangent σ_t components [15, 16]:

$$\sigma = \sqrt{\sigma_r^2 + \sigma_t^2} \tag{1}$$

$$\sigma_r = \frac{3 \cdot P}{8 \cdot h^2} \cdot (a^2 \cdot (1 + \mu) - r^2 \cdot (3 + \mu)) \tag{2}$$

$$\sigma_t = \frac{3 \cdot P}{8 \cdot h^2} \cdot (a^2 \cdot (1 + \mu) - r^2 \cdot (1 + 3 \cdot \mu)) \tag{3}$$

where a is radius of membrane, h is thickness of membrane, r – is distance from center of membrane, μ is Poisson's ratio of membrane material.

 978-1-7281-0339-6/19/$31.00 ©2019 IEEE

$$\sigma_r^2 = \left(\frac{3P}{8h^2}\right)^2 \cdot \left(a^4 \cdot (1+\mu)^2 - 2a^2 \cdot (1+\mu) \cdot r^2 \cdot (3+\mu) + r^4 \cdot (3+\mu)^2\right) \quad (4)$$

$$\sigma_\theta^2 = \left(\frac{3P}{8h^2}\right)^2 \cdot \left(a^4 \cdot (1+\mu)^2 - 2a^2 \cdot (1+\mu) \cdot r^2 \cdot (1+3\mu) + r^4 \cdot (1+3\mu)^2\right) \quad (5)$$

$$\sigma^2 = \left(\frac{3P}{8h^2}\right)^2 \cdot \left((2a^4(1+\mu)^2 - 2a^2(1+\mu)r^2(1+4\mu) + r^4((3+\mu)^2 + (1+2\mu)^2)\right) \quad (6)$$

$$\sigma^2 = \left(\frac{3P}{8h^2}\right)^2 \cdot \left((1+\mu)^2 \cdot (2a^4 - 8a^2r^2) + r^4 \cdot (9+6\mu+\mu^2+1+6\mu+9\mu^2)\right) \quad (7)$$

$$\sigma^2 = \left(\frac{3P}{8h^2}\right)^2 \cdot \left((1+\mu)^2 \cdot (2a^4 - 8a^2r^2) + r^4 \cdot (10+12\mu+10\mu^2)\right) \quad (8)$$

$$\sigma = \frac{3P}{8h^2} \cdot \sqrt{\left((1+\mu)^2 \cdot (2a^4 - 8a^2r^2) + r^4 \cdot (10+12\mu+10\mu^2)\right)} \quad (9)$$

Maximum mechanical stresses ($\sigma=\sigma_{max}$) occur when the distance from center of membrane is equal to the radius of the membrane ($r = a$):

$$\sigma_{max} = \frac{3P}{8h^2} \cdot \sqrt{\left((1+\mu)^2 \cdot (-6a^4) + a^4 \cdot (10+12\mu+10\mu^2)\right)} \quad (10)$$

$$\sigma_{max} = \frac{3P}{8h^2} \cdot \sqrt{a^4 \cdot (-6-12\mu-6\mu^2+10+12\mu+10\mu^2)} \quad (11)$$

$$\sigma_{max} = \frac{3 \cdot P \cdot a^2}{4 \cdot h^2} \cdot \sqrt{1+\mu^2} \quad (12)$$

Next, we introduce a variable $B(\mu)= \frac{3}{4}\sqrt{1+\mu^2}$. The final equation allows us to establish an analytical relationship between excess pressure on membrane P and maximum mechanical stress σ_{max} shown below (13):

$$\sigma_{max} = \frac{P \cdot a^2}{h^2} \cdot B(\mu) \quad (13)$$

The developer can calculate the critical excess pressure on the membrane element of device from equation (13) by substituting into the equation thickness of the membrane h, the radius of the membrane a, the maximum mechanical stress σ_{max} equal to the mechanical strength of the material and variable $B(\mu)$.

III. Experiment

The process of manufacturing membranes was carried out through the formation of cavities in silicon wafers in the Bosch process. The plasma-chemical process (Bosch) is characterized by a higher anisotropy and accuracy of the formation of elements compared with the liquid method of etching silicon. In addition, the etching rate reaches 10 μm / min and does not depend on the crystallographic orientation of the substrate. This allows the membrane to form within a few hours. As a mask, a layer of aluminum was used, which was applied on the reverse side of the substrate (Fig. 1). The formation of layers of aluminum film was carried out by magnetron sputtering on the installation MAGNA. The surface was treated with an ion beam (argon ions) with a power of 120 W and an energy of 300 eV after applying a single layer.

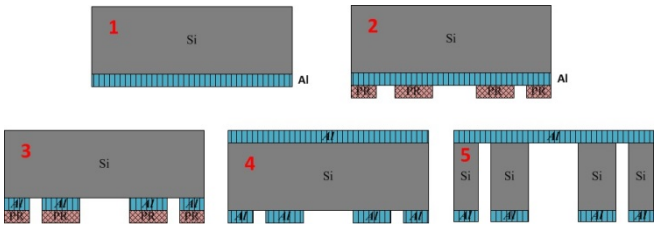

Fig.1. Stages 1-5 of the technological route of membrane formation

As can be seen from the figure above, membranes with perforated areas of low mechanical strength were formed during the final fifth stage of the technological route. The perforated areas are either closed due to liquid etching in a special cassette [17] or they form cracks along the perforation line by means of manual mechanical action. This eliminates the standard automatic cutting of the substrate on the crystals and prevents the ingress of elements from the diamond disc, which lead to critical deformation of the structure in the region of the membrane.

IV. Measurement of Membrane Parameters

Aluminum membranes consisting of a continuous layer, 10 layers, 20 layers and 30 layers were formed during the technological route. The result of measuring the total thickness of the films of the above samples using a scanning electron microscope (SEM) Quanta 3D FEI is shown in Fig. 2 and 3 below.

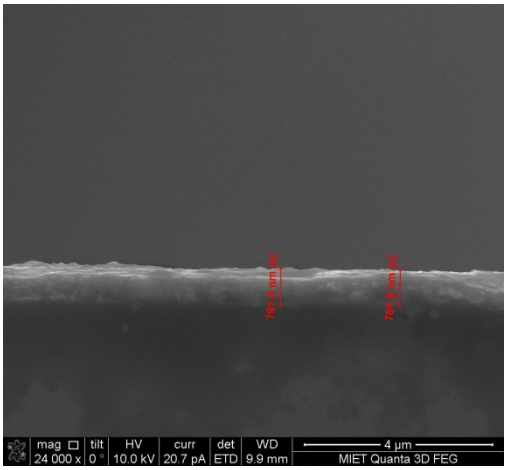

Fig.2 Control of the thickness of 20 layers of aluminum by SEM

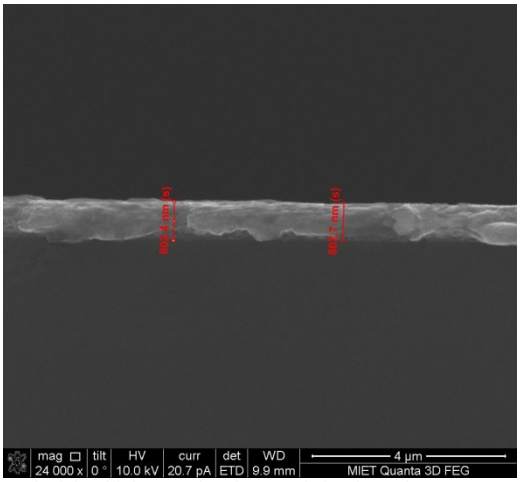

Fig.3 Control of the thickness of 30 layers of aluminum by SEM

Next, the samples were studied by the method of secondary ion mass spectrometry using a ToF.SIMS 5–100 time-of-flight mass spectrometer by the German company ION-TOF. The energy of the analytical beam Bi + was 30 keV. The sputtering was carried out with Cs + ions with an energy of 2 keV in the analysis of negative secondary ions. Spraying craters measured 300 × 300 microns. Ions from the central region of the crater 100 × 100 µm in size coinciding with the contact window were used for analysis. The etching crater depth was measured using an AlphaStep profilometer, after which the etching time was recalculated into depth. The distribution profiles of the elements in the studied samples are shown in Fig.4. The current of the molecular ion AlSi– was measured together with the currents of the atomic ions H–, C–, O–, Al– and Si–. The maximum current of this ion corresponds to the interface between the aluminum layer and the silicon substrate. The result of measuring two types of film thickness using a time-of-flight mass spectrometer is presented in Fig. 4 and 5 below.

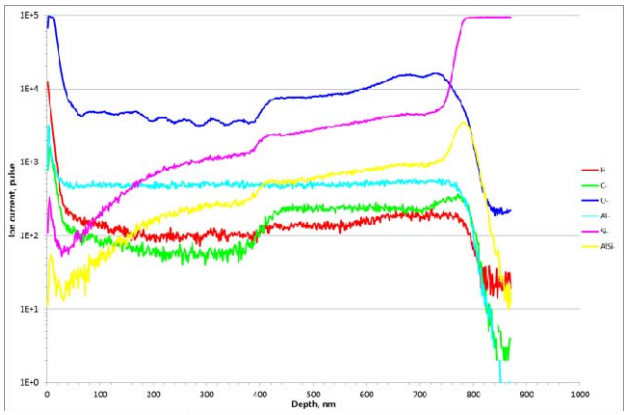

Fig.4 Control of the thickness of 20 layers of aluminum by means of SIMS

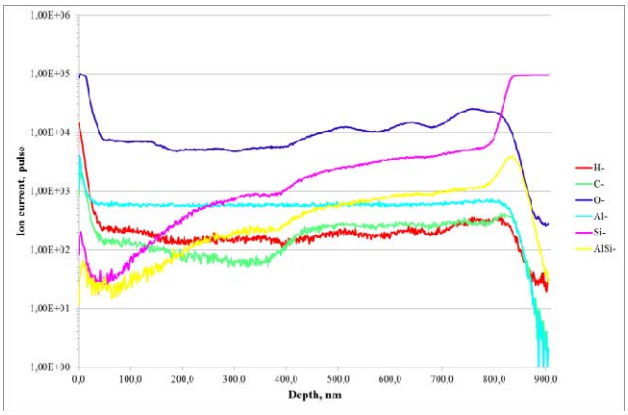

Fig.5 Control of the thickness of 30 layers of aluminum by means of SIMS

Next, Fig. 6 presents a graph of the distribution of oxygen in a 10-layer aluminum structure.

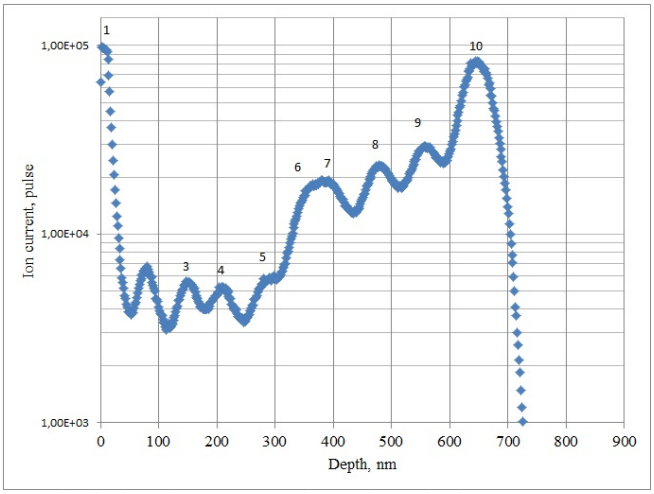

Fig.6. Distribution of oxygen atoms in a 10-layer aluminum structure

It can be concluded, that a good correlation of the results of measuring the thickness of aluminum is observed using a scanning electron microscope and a time-of-flight mass spectrometer. Analyzing the oxygen peaks it can be concluded that the Al structure consists of 10 layers. The thickness of the continuous layer of aluminum is 1340 ± 10 nm, the total thickness of 10 layers is 700 ± nm, 20 layers of 780 ± 10 nm, and 30 layers of 800 ± 10 nm.

Next, the roughness measurement of the samples was performed on an AIST-NT SmartSPM 1000 atomic force microscope. Fig. 7 shows a three-dimensional image of the relief on a scan area of 20 × 20 µm^2.

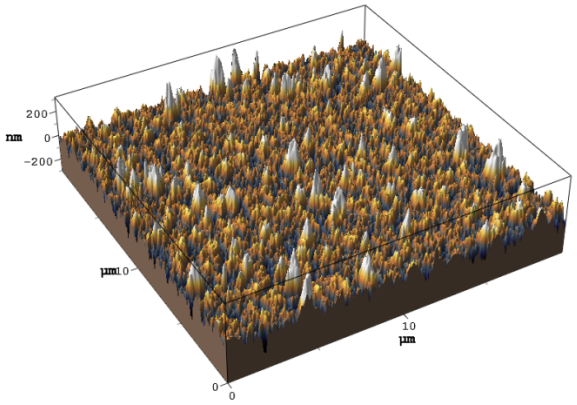

Fig.7 Surface relief of the aluminum membrane

Next, Fig. 8 shows the dependence of the surface roughness of the aluminum membrane (arithmetic average deviation of the Ra profile) on the number of layers. The given dependence visually proves that with an increase in the number of aluminum layers, the total exposure time to the structure increases linearly, which leads to an increase in roughness.

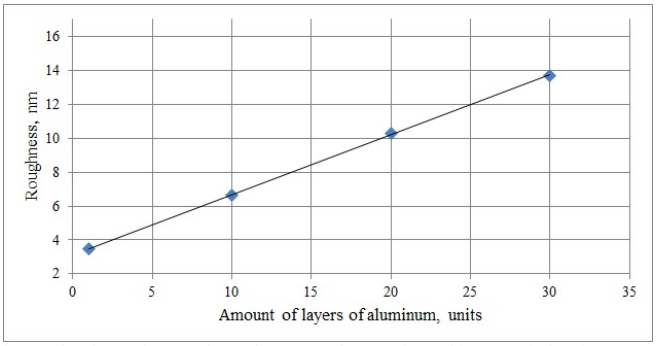

Fig.8. The dependence of roughness on the number of layers of aluminum

V. Measurement of Mechanical Strength

The following results were obtained on a previously developed stand for determining mechanical strength by bulge method [18]. The accuracy of manometer is ± 0.05 atm. The aluminum membrane with a diameter of 1.0 mm, which is a continuous layer 1340 ± 20 nm thick, withstands an excess pressure of at least 5.8 atm. The dependence of deflection of membrane *w* from excess pressure *P* shown on Fig.9.

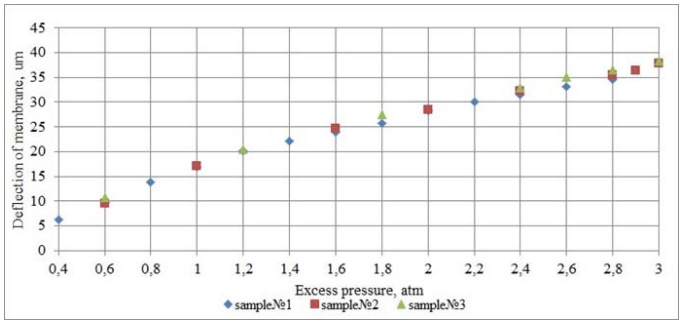

Fig.9. The dependence of deflection of membrane from excess pressure

We had good correlation *w*(*P*) from different samples.

The structure consisting of 10 layers with a total thickness of 700 ± 10 nm, withstands a critical excess pressure from 2.0 to 2.4 atm at Ø1.0 mm, and critical excess pressure from 2.7 to 3.3 atm at Ø 0.75 mm.

The sample, which is 20 layers with a total thickness of 780 ± 25 nm, with overstay from 2.0 to 2.1 atm at Ø1.0 mm, and critical excess pressure from 2.7 to 3.3 at a diameter 0.75 mm.

The structure, consisting of 30 layers with a total thickness of 800 ± 10 nm, withstands critical excess pressure of 2.1 atm at Ø1.0 mm, and critical excess pressure from 2.7 to 3.2 atm at Ø0.75 mm.

From Fig. 10, distribution of mechanical stresses over the diameter of the membrane is shown by equation (9). Poisson's ratio of aluminum is 0.34.

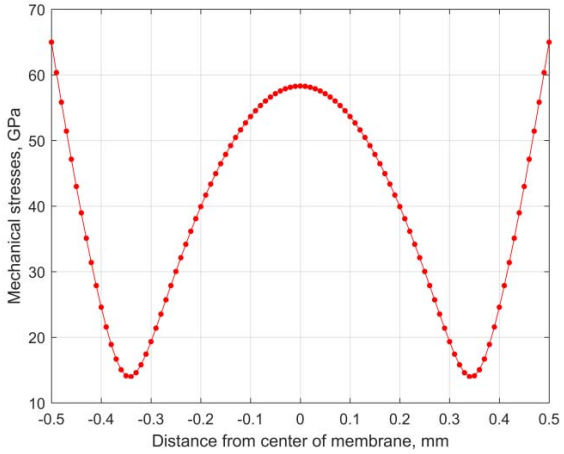

Fig.10. Distribution of mechanical stresses along diameter of membrane of 800 nm thickness

Maximum mechanical stresses occur at the membrane – substrate interface. The next step (Fig.11) was the calculated value of the mechanical strength of the membranes (maximum mechanical stresses) by equation (13).

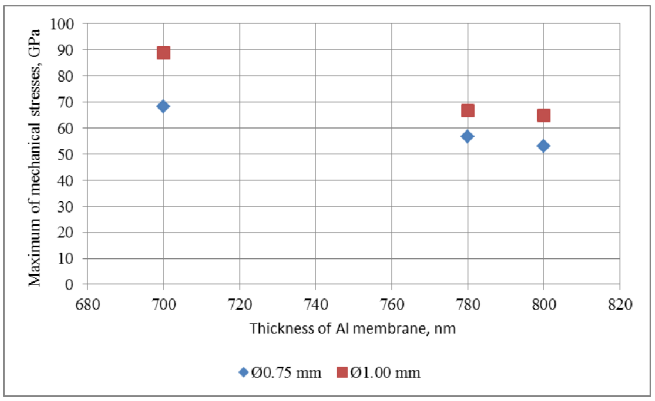

Fig.11. Dependence of maximum mechanical stresses from membrane thickness

It is noticeable that value of the maximum mechanical stresses decreases with increasing membrane thickness. The difference of maximum mechanical stresses in 10 (700nm) and 20 (780nm) layers is much more than in 20 and 30 (800nm)

layers. Therefore, the factor of the membrane layer thickness significantly affects the mechanical strength than the etching time factor. Consequently, values of maximum mechanical stresses will be less for millimeter ("thick") layers of materials used in airplanes and spacecraft. The standard values of mechanical strength of aluminum alloys vary in the range from 90 to 570 MPa, and depend on technology of layer formation [19–22]. The mechanical strength of the aluminum material is increased by doping with atoms of copper, zinc, magnesium, manganese, and silicon. Another way to increase the strength of aluminum is the creation of plastic (inelastic) deformation due to thermal processing, which creates dislocations in the aluminum crystal lattice. Dislocations increasingly collide with each other with increasing plastic strain values. As a result, the resistance to further deformation increases, therefore, the strength increases. Operations are performed with higher accuracy in microelectronics, so it is possible to get a greater effect with a similar technology.

The specific strength of the material of the membrane can be estimated by the ratio of the maximum stresses σ_{max} to the thickness of membrane h. For example, ratio σ_{max}/h varies from 6.64 to 9.74 × 10^{16} Pa/nm with a thickness of 800 (30 layers) to 700 nm (10 layers) for a diameter of 0.75 mm. A similar relationship was observed for a diameter of 1.0 mm. The total exposure time of the ion gun increases with increasing number of layers. Thus, value of specific strength of the material decreases with an increase in the exposure time of the ion gun.

Next, samples with a continuous layer and a 10-layer structure were subjected to ion beam etching in an argon atmosphere for 22 minutes at a power of 500 W and an energy of 500 eV. An aluminum membrane with a diameter of 1.0 mm, which is a continuous layer 1100 ± 30 nm thick (after etching), withstands an overpressure of 3.1 atm. An aluminum membrane with a diameter of 1.0 mm and a thickness of 550 ± 30 nm, which is a set of layers, withstands an excess pressure of 0.55 atm. Confirmed, that bombardment of the surface with ions reduces the mechanical strength of the structures by several times.

VI. CONCLUSIONS

There is a good correlation between the results of measuring the thickness of aluminum using a scanning electron microscope and a secondary ion mass spectrometer. Borders between single layers of aluminum are determined by oxygen peaks. It has been experimentally determined that ion-beam etching increases the structure roughness, which reduces the mechanical strength of aluminum membranes several times. The developer can calculate the critical excess pressure on the membrane element of device from equation (13) by substituting into the equation thickness of the membrane h, the radius of the membrane a, the maximum mechanical stress σ_{max} equal to the mechanical strength of the material and variable $B(\mu)$.

ACKNOWLEDGMENT

This work was carried out on the equipment of the R&D center "MEMS and electronic components" and supported by Ministry of Education and Science of Russian Federation (within the agreement № 14.578.21.0250, id RFMEFI57817X0250)

REFERENCES

[1] C. Kilpatrick "X-ray limits on the progenitor system of the Type Ia supernova" in Monthly Notices of the Royal Astronomical Society, 481 (3), pp. 4123-4132, 2018

[2] D. Stupple, V. Kemp, M. Oldfield, J. Watts and M. Baker, "Modeling of Heat Transfer in an Aluminum X-Ray Anode Employing a Chemical Vapor Deposited Diamond Heat Spreader" in Journal of Heat Transfer, 140 (12), № 124501, 2018

[3] B. Kozioziemski, "An x-ray optic calibration facility for high energy density diagnostics" Review of Scientific Instruments, 89 (10), № 10G112, 2018

[4] Y. Kessler, B. Ilic, S. Krylov and A. Liberzon, "Flow Sensor Based on the Snap-Through Detection of a Curved Micromechanical Beam" in Journal of Microelectromechanical Systems, 2018

[5] M. Horning, R. Shakya and N. Ida, "Design of a Low-Cost Thermal Dispersion Mass Air Flow (MAF) Sensor" in Sensing and Imaging, 19 (1), № 21, 2018

[6] M. Islam, "A prominent smart gas meter" in 2018 2nd International Conference on Electronics, Materials Engineering and Nano-Technology, IEMENTech, 2018

[7] E. Sugata, H. Yokoya and K. Kitakaze, "The mechanical strength of thin films under electron bombardment" in Journal of Electronmicroscopy, vol.7, p.19-20, 1959

[8] K. Takahata "Micro Electronic and Mechanical Systems", 386 p., 2009

[9] N. Liakishev and M.Alimov, "Constructional Nanomaterials" in Russian Nanotechnologies, vol. 1, 2006

[10] Y.-G. Jung, A. Pajares, and B. R. Lawn, "Effect of oxide and nitride films on strength of silicon: a study using controlled small-scale flaws" in J. Mater. Res., vol. 19, No. 12, Dec 2004

[11] I. Ganutdinov, E. Nesmelov, and R. Aliakberov, "Method of estimating the mechanical strength of thin-film coatings" in J. Opt. Technol. 71 (8), August 2004

[12] A. Vlasov, T. Civinskaya and A. Shahnov "Analysis of the influence of the shape of the membrane on the mechanical strength and stability of the parameters of MEMS pressure sensors" , MES-2016

[13] R. Siegel and G. Fougere, "Mechanical properties of nanophase metals", Nanostr. Mat, vol. 6, № 1—4. p. 205, 1995

[14] E. Ovidko and E. Gutkin, "Physical mechanics of deformable nanostructures" in Nanocrystalline materials, vol. I, St. Petersburg. Janus 2003

[15] I. Barinov and V. Volkov, "Sensitive elements of micromechanical pressure sensors", Fundamentals of design and development, 2013, 79 p., Penza.

[16] S. Timoshenko and S. Voinovsky-Krieger "Records and shells", Study Guide. - M .: Science, 1966. - 635 p.

[17] N. Djuzhev and E. Gusev, "A device for the chemical separation of semiconductor wafers into crystals" Patent of the Russian Federation for invention № 2664882, 2017

[18] E. Gusev, A. Dedkova and N. Djuzhev, "Investigation of the mechanical strength of multilayer membranes for MEMS transducers of physical quantities" in Nanoindustry, №82, p.538-541, 2018

[19] A. Abdullah, "Mechanical Properties of Materials(Aluminium, Stainless Steel, C-Steel) ", Qatar University, 2014.

[20] W. Callister, "Materials Science and Engineering: An Introduction", 7th edition. John Wiley & Sons, Inc., 2007

[21] R. Nunes et al., "Properties and Selection: Nonferrous Alloys and Special-Purpose Materials", Metals Handbook, ASM International, Vol.2, 10th Ed. 1990.

[22] P. Summers et al., «Overview of aluminum alloy mechanical properties during and after fires», Fire Science Reviews, Springer, 2015.